Distinct Cardiac Connexin-43 Expression in Hypertrophied and Atrophied Myocardium May Impact the Vulnerability of the Heart to Malignant Arrhythmias. A Pilot Study

Barbara SZEIFFOVA BACOVA[1], Katarina ANDELOVA[1], Matus SYKORA[1], Tamara EGAN BENOVA[1], Lin Hai KURAHARA[2], Jan SLEZAK[1], Narcis TRIBULOVA[1]

[1]Centre of Experimental Medicine, Slovak Academy of Sciences, Bratislava, Slovak Republic, [2]Department of Cardiovascular Physiology, Faculty of Medicine, Kagawa University, Kagawa, Japan

Received September 2, 2022
Accepted November 8, 2022

Summary

Our and other studies suggest that myocardial hypertrophy in response to hypertension and hyperthyroidism increases propensity of the heart to malignant arrhythmias, while these are rare in conditions of hypothyroidism or type-1 diabetes mellitus associated with myocardial atrophy. One of the crucial factors impacting the susceptibility of the heart to life-threatening arrhythmias is gap junction channel protein connexin-43 (Cx43), which ensure cell-to-cell coupling for electrical signal propagation. Therefore, we aimed to explore Cx43 protein abundance and its topology in hypertrophic and hypotrophic cardiac phenotype. Analysis were performed in left ventricular tissue of adult male spontaneously hypertensive rat (SHR), Wistar Kyoto rats treated for 8-weeks with L-thyroxine, methimazol or strepotozotocin to induce hyperthyroid, hypothyroid and type-1 diabetic status as well as non-treated animals. Results showed that comparing to healthy rats there was a decrease of total myocardial Cx43 and its variant phosphorylated at serine368 in SHR and hyperthyroid rats. Besides, enhanced localization of Cx43 was demonstrated on lateral sides of hypertrophied cardiomyocytes. In contrast, total Cx43 protein and its serine368 variant were increased in atrophied left ventricle of hypothyroid and type-1 diabetic rats. It was associated with less pronounced alterations in Cx43 topology. In parallel, the abundance of PKCε, which phosphorylates Cx43 at serine368 that stabilize Cx43 function and distribution was reduced in hypertrophied heart while enhanced in atrophied once. Findings suggest that differences in the abundance of cardiac Cx43, its variant phosphorylated at serine368 and Cx43 topology may explain, in part, distinct propensity of hypertrophied and atrophied heart to malignant arrhythmias.

Key words

Connexin-43 • PKCε • Rat heart • Myocardial hypertrophy • Myocardial atrophy

Corresponding author

N. Tribulová, Centre of Experimental Medicine, Slovak Academy of Sciences, 841 04 Bratislava, Slovak Republic. E-mail: narcisa.tribulova@savba.sk

Introduction

The heart is electro-mechanical pump and contractile work of cardiomyocytes largely determine cardiomyocyte size. Thus, changes in hemodynamic load cause alterations in cardiomyocyte size, with regional variations in distribution [1]. Structural remodelling of cardiomyocytes is a major component in both cardiac hypertrophy and atrophy in response to increased or decreased workloads [2,3]. Volume overload is generally associated with eccentric hypertrophy and increased cardiomyocyte length being the predominant feature. Pressure overload generally results in concentric hypertrophy characterized by increased cardiomyocyte cross-sectional area. A combined volume and pressure overload can be produced by administration of thyroid hormone, with increased the length and cross-sectional area of cardiomyocytes [1]. Conversely, structural

© 2023 by the authors. Published by the Institute of Physiology of the Czech Academy of Sciences, Prague, Czech Republic

remodelling of cardiomyocytes leading to decreased cardiomyocyte size and atrophy can be elicited by a reduction in afterload or in mechanically unloaded heart [4]. This is the case of thyroid hormone deficiency [5] and type-1 diabetes mellitus (T1DM) due to an increase deiodinase-3 that converts both thyroxine and active triiodothyronine into inactive metabolites [6].

In the context of cardiomyocyte size it is interesting the fact implying from experimental and clinical studies that myocardial hypertrophy due to hypertension or hyperthyroidism increases susceptibility of the heart to malignant arrhythmias [7-9], while myocardial atrophy due to T1DM or hypothyroidism renders the heart less prone to develop life-threatening ventricular arrhythmias [9-12]. Thus, to identify the abnormal substrate as a major culprit for sustained ventricular arrhythmias jeopardizing cardiac hemodynamic is relevant.

One of the crucial factors determining susceptibility of the heart to malignant arrhythmias is connexin-43 (Cx43), the dominant cardiac protein of gap junction channels, which ensure electrical coupling for action potential propagation among cardiomyocytes [13,14]. Variations in cardiomyocyte coupling due to amount and alterations of Cx43 channels as well as their topology can account for variations in conduction velocity and non-uniform anisotropy, while Cx43 channels uncoupling slows or even blocks conduction of electrical impulse [15,16]. Thus, loss of Cx43 and changes in its conventional cardiomyocyte topology perturb myocardial anisotropic electrical conduction and predispose to life-threatening arrhythmias [14,17]. Those, like ventricular fibrillation and high frequency tachycardia occur due to conduction block followed by re-entry of excitation [18]. Function of Cx43 channels is controlled by complex and multifactorial processes, including their phosphorylation [13,14]. It is noteworthy that the increased level of Cx43 variant phosphorylated at serine368 by PKCε, stabilizes channels, prevents lateralization and attenuates Cx43 channel conductivity [19]. These effects can contribute to maintenance of anisoptropic cardiac conduction.

The present study was undertaken to explore whether the abundance of Cx43, its localization in cardiomyocytes as well as serine368 Cx43 variant along with PKCε differ in hypertrophied and atrophied heart that may contribute to distinct propensity to malignant arrhythmias. We used two established models of cardiac hypertrophy and two models of cardiac atrophy, i.e. spontaneously hypertensive rats, hyperthyroid rats, hypothyroid and type-1 diabetic rats.

Material and Methods

Animal models

Male, adult Wistar Kyoto rats (WKY) and spontaneously hypertensive rats (SHR) were used throughout experiments that were approved by our Institution's Animal Care and Use Committee and in accordance with the "Guide for the Care and Use of Laboratory Animals" published by USA National Institutes of Health (NIH publication No 85-23, revised 1996). Hyperthyroid status was elicited in WKY rats by daily treatment with intraperitoneal injection of 3,3',5-triiodo-L-thyronine (Sigma Aldrich, Missouri, USA; 0.15 μg/kg b.w. for eight-weeks). Hypothyroid status was elicited by daily treatment of WKY rats with 0.05 % solution of methimazole (Sigma Aldrich, Missouri, USA) in the drinking water for eight-weeks. Type-1 diabetes mellitus was elicited in WKY rats by single intravenous injection of streptozotocin (STZ, Sigma Aldrich, Missouri, USA; 50mg/kg b.w.) and examined eight-weeks later. Animals were divided into following groups: SHR, (n=6); Hyperthyroid rats (HT, n=6); Hypothyroid rats (HY, n=6); Type-1 diabetes mellitus rats (T1DM, n=6). Besides, WKY (n=12) served as a healthy control. At the end of the experiment rats were euthanized by overdose ketamine (100 mg/kg b.w. of Narketan; Vetoquinol UK Ltd., Towcester, UK). After blood collection, the heart was quickly excised into ice-cold saline to stop contraction followed by dissection and registration of heart and left ventricular weights. Myocardial tissue was snap frozen in liquid nitrogen and tissue as well as fasting blood serum samples were stored in a freezer at -80 °C until use for analysis.

Blood serum and myocardial tissue analysis

Blood glucose level was registered using the EasyGluco system. Serum levels of total L-thyroxine (T4) and 3,3',5-triiodo-L-thyronine (T3) were determined using commercial RIA kits (Immunotech/Beckman Coulter Co., Prague, Czech Republic).

Cardiomyocyte hypertrophy and atrophy was determined by measurement of cross-sectional area (CSA) in transverse cardiomyocytes, in tissue sections stained with haematoxylin-eosin and examined in Apotome 2 microscope (Carl Zeiss Microscopy GmbH, Jena, Germany) at 40× magnification. CSA was

evaluated in digitalized microscopic images using ZEN 2.5 software (Carl Zeiss Microscopy GmbH, Jena, Germany). About 15-20 cardiomyocytes were scored in each tissue section per heart (n=6 rats in each group).

In situ immunolabeling of Cx43 was performed on 10 μm-thick cryosections as previously described [20]. After fixation in ice-cold methanol and blocking with 1 % BSA section were incubated overnight with primary anti-Cx43 antibody (diluted 1:500, MAB3068, CHEMICON International, Inc., Temecula, CA, USA), washed in PBS and incubated with secondary antibodies conjugated with FITC-fluorescein isothiocyanate (diluted 1:500, Jackson Immuno Research Labs, West Grove, PA, USA). Immunostaining was examined in Zeiss Apotome 2 microscope (Carl Zeiss Microscopy GmbH, Jena, Germany) and acquired microscopic images were used for quantitative analysis of Cx43 distribution on lateral sides of the cardiomyocytes. Quantification of Cx43 lateralization, was performed in the 7 test field per slice and analysed using Image-Pro Plus software as previously described in details [21]. The lateral Cx43 topology was expressed as a percentage calculated from the ratio of integral optical density (IOD) of lateral topology divided by the total IOD.

SDS-PAGE and Western blot analysis of Cx43 and PKC proteins in left heart ventricles were determined as previously described [22]. Transferring the proteins to a nitrocellulose membrane was followed by incubation overnight with primary antibodies: anti-total-Cx43 (diluted 1:5000, C6219, Sigma-Aldrich, Missouri, USA) and anti-phospho-serine 368-Cx43 (diluted 1:1000, sc-101660, Santa Cruz Biotechnology, Texas, USA) as well as anti-PKCε (diluted 1:1000, sc-214, Santa Cruz Biotechnology, Texas, USA). Besides, anti-GAPDH (diluted 1:1000, sc-25778, Santa Cruz Biotechnology, Texas, USA) detection was performed for using as a housekeeping protein. The membranes were subsequently washed in TBST and incubated for 1 h with a horseradish peroxidase-linked secondary antibodies (diluted 1:2000, #7074/#7076, Cell Signalling Technology, Colorado, USA). The proteins were visualized *via* electrochemiluminescence followed by densitometry using Carestream Molecular Imaging Software (version 5.0, Carestream Health, New Haven, Connecticut, USA).

Differences between groups were statistically evaluated using one-way analysis of variance (ANOVA) and Bonferroni's multiple comparison test. The Kolmogorov-Smirnov normality test reveal the normal distribution of variables. Data were expressed as means ± standard deviation (SD); $p<0.05$ was considered to be significant.

Results

Registered characteristics of experimental rats shown in Table 1 demonstrate that comparing to healthy WKY rats the body weight was significantly reduced in SHR and T1DM rats. Heart weight and left ventricular weight were significantly increased in SHR and hyperthyroid rats, whereas decreased in hypothyroid and T1DM rats. Hypertrophic and atrophic cardiac phenotype was confirmed by significant increase of cross sectional cardiomyocyte diameter in SHR and hyperthyroid rats and decrease in hypothyroid and T1DM rats when compared to healthy WKY rats. Moreover, the changes in serum levels of T4, T3 and blood glucose pointed out hyperthyroid, hypothyroid and diabetic status in corresponding rats group.

Table 1. Biometric parameters, blood serum glucose and thyroid hormones in experimental rats.

	C	TH	SHR	HY	T1DM
BW (g)	411.1 ± 37.2	412.0 ± 42.4	317.2 ± 23.4*	403.6 ± 14.3	342.5 ± 34.1*
HW (g)	1.04 ± 0.13	1.69 ± 0.12*	1.35 ± 0.13*	0.76 ± 0.08*	0.78 ± 0.16*
LVW (g)	0.79 ± 0.12	0.98 ± 0.05*	0.98 ± 0.12*	0.57 ± 0.02*	0.62 ± 0.09*
CSA (μm^2)	311.9 ± 48.7	710.9 ± 56.2*	759.2 ± 97.5*	227.2 ± 24.9*	214.8 ± 38.3*
BG (nmol/l)	4.83 ± 0.80	5.02 ± 0.05	5.95 ± 0.07	4.09 ± 0.95	25.85 ± 4.25*
T3 (nmol/l)	0.86 ± 0.21	2.30 ± 0.72*	0.92 ± 0.22	0.58 ± 0.09*	0.62 ± 0.05*
T4 (nmol/l)	53.91 ± 12.30	105.56 ± 26.05*	40.17 ± 11.25	16.87 ± 1.05*	27.50 ± 1.75*

BW – body weight, HW – heart weight, LVW – left ventricular weight, CSA – cross sectional area, BG – blood glucose, T3 – 3,3',5-triiodo-L-thyronine, T4 – L-thyroxine. * $p<0.05$ vs. control.

Western blot analysis revealed that total Cx43 protein levels as well as its variant phosphorylated at serine368 are significantly reduced in hypertrophied left ventricle of SHR and hyperthyroid rat hearts compared to healthy rats (Fig. 1A, B). In parallel, myocardial protein levels of PKCε were decreased in these rats when compared to healthy (Fig. 1C).

In situ immunolabeling of Cx43 in left ventricular tissue followed by quantitative image analysis pointed out lower immunopositivity in SHR and hyperthyroid rat hearts (Fig. 2). However, besides conventional localization Cx43 at the intercalated discs (end-to-end type), there was apparently enhanced immunopositivity on lateral plasma membrane of the cardiomyocytes. This "lateralization" (side-to-side type) was significant comparing to healthy rat hearts.

On the other hand, abundance of Cx43, including its serine368 variant were significantly increased in left ventricle of hypothyroid and T1DM rats (Fig. 3A, B). Likewise, there was an increase of PKCε protein levels (Fig. 3C).

Moreover, significant increase of Cx43 immunopositivity at the intercalated discs was found in ventricular tissue sections, while "lateralization", i.e. amount of Cx43 on lateral sides of the cardiomyocytes was not significant (Fig. 4) when comparing to healthy rats.

According to Kolmogorov-Smirnov normality test there was normal distribution of the data.

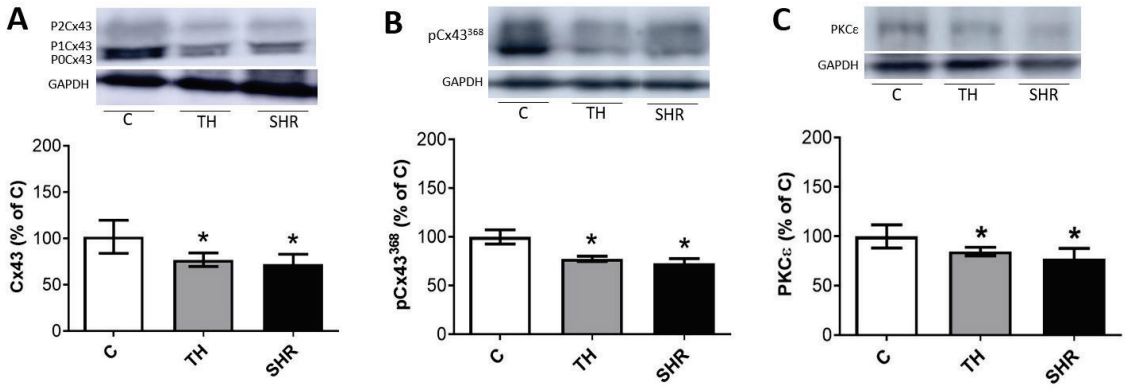

Fig. 1. Representative images of Western blots and quantitative assessment of: (**A**) total protein levels of Cx43; (**B**) Cx43 variant phosphorylated at serine368; (**C**) PKCε protein levels in the left ventricle of hyperthyroid (TH) and spontaneously hypertensive (SHR) rats compared to healthy control rats (C). Values are mean ± SD, (n=6 in each group), * p<0.05 vs. control.

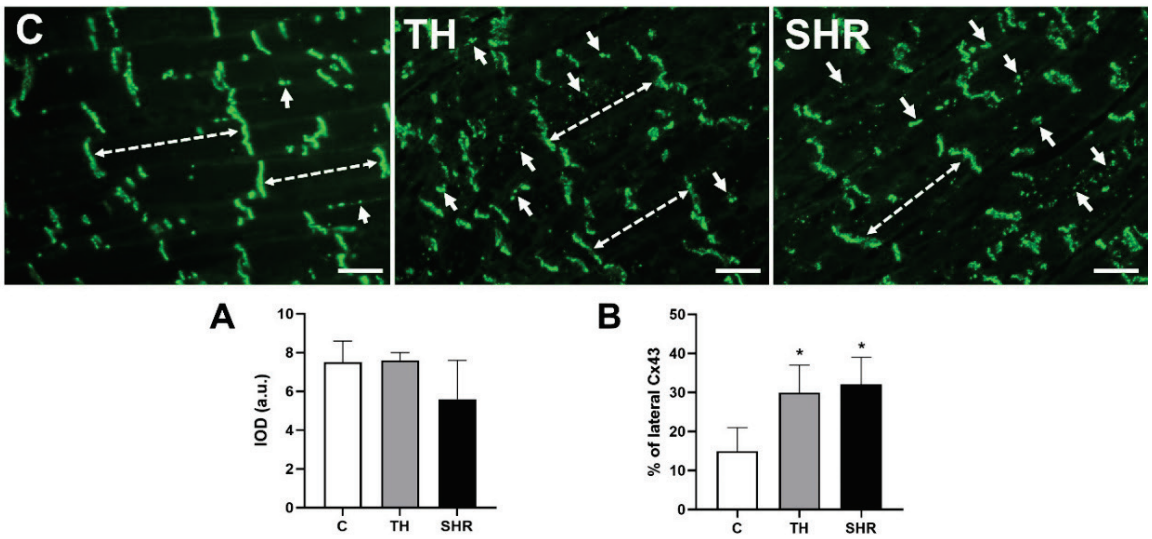

Fig. 2. The representative microscopic images of Cx43 imunolabeling (green color) in longitudinally apposed left ventricular cardiomyocytes of experimental rats. Note the prevalent end-to-end type (broken arrows) of Cx43 distribution at the intercalated discs and sporadically at the lateral sides (arrowheads) of the cardiomyocytes in healthy rats (**C**). In contrast to the reduced total Cx43 imunolabeling (**A**) its lateral distribution is enhanced in hyperthyroid rats (TH) and SHR left heart ventricles as assessed by quantitative image analysis (**B**). Scale bar represents 100 μm. Values are mean ± SD, (n=6 in each group), * p<0.05 vs. control.

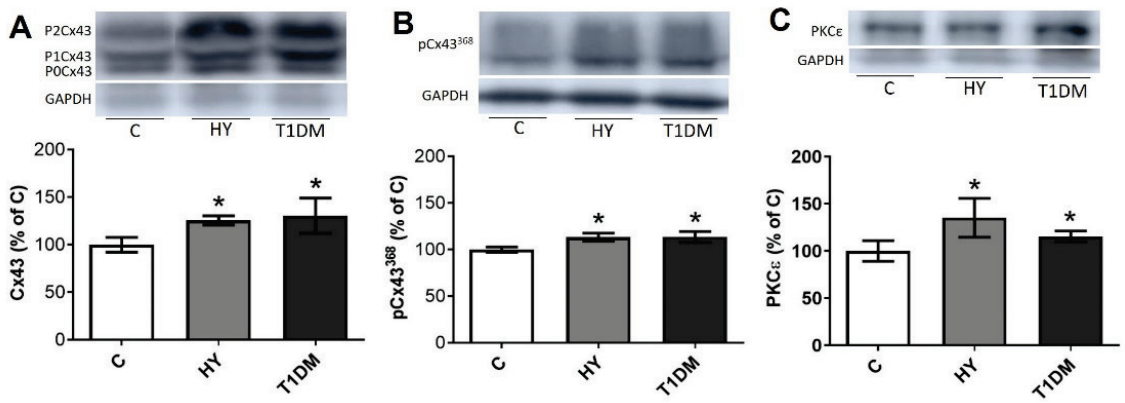

Fig. 3. Representative images of Western blots and quantitative assessment of: (**A**) total protein levels of Cx43; (**B**) Cx43 variant phosphorylated at serine368; (**C**) PKCε protein levels in the left ventricle of hypothyroid (HY) and type-1 diabetic (T1DM) rats compared to healthy control rats (C). Values are mean ± SD, (n=6 in each group), * p<0.05 vs. control.

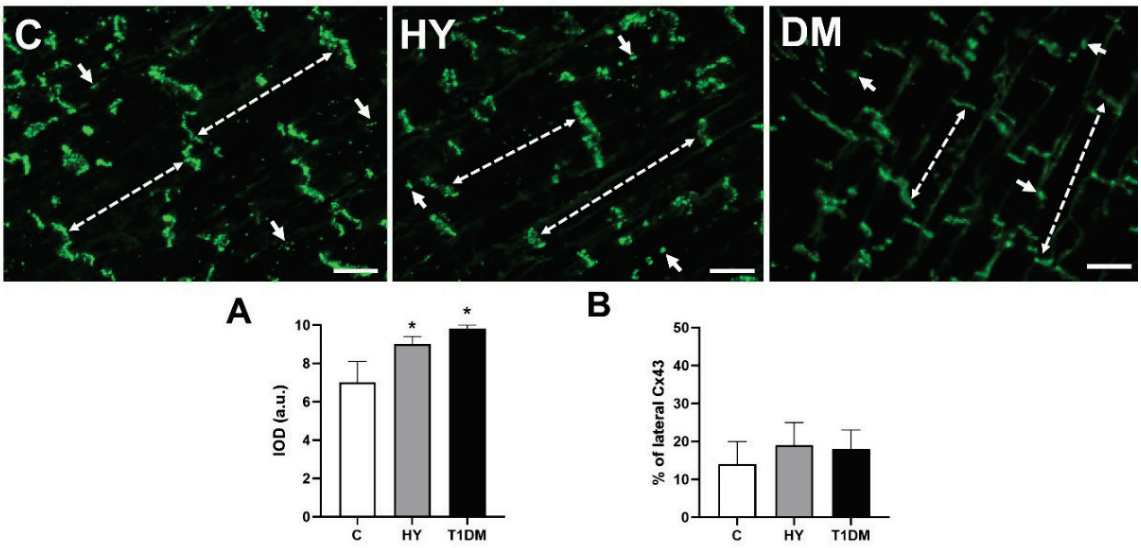

Fig. 4. The representative microscopic images of Cx43 imunolabeling (green color) in longitudinally apposed left ventricular cardiomyocytes of experimental rats. Note the prevalent end-to-end type (broken arrows) Cx43 distribution at the intercalated discs and sporadically at lateral sides (arrowheads) of the cardiomyocytes in healthy rats (**C**) as well as in hypothyroid (HY) and type-1 diabetic rats (T1DM). Total Cx43 imunolabeling (**A**) was increase while not its lateral distribution in HY and T1DM rat heart left ventricles as assessed by quantitative image analysis (**B**). Scale bar represents 100 μm. Values are mean ± SD, (n=6 in each group), * p<0.05 vs. control.

Discussion

The current study strongly points out that adaptive responses to cardiac load induces either myocardial hypertrophy due to increase workload in SHR and hyperthyroid rats or myocardial atrophy due to decrease workload in hypothyroid and type-1 diabetic rats. We have demonstrated that myocardial structural remodelling in regard to the cardiomyocyte size affects both abundance and topology of principal gap junction channel protein, Cx43. Accordingly, the left ventricular hypertrophy in SHR and hyperthyroid rats was accompanied by down/regulation and miss-localization of Cx43, while myocardial atrophy in hypothyroid and type-1 diabetic rats was associated with upregulation of Cx43 and minor alterations in its topology.

Data in literature point out that myocardial structural remodelling and impairment of Cx43 mediated cardiomyocyte communication impact both heart function [1,23] and susceptibility of the heart to arrhythmias [18,24]. In line with current findings, down-regulation and altered topology (lateralization) of Cx43 in left heart ventricle of hypertensive or hyperthyroid rats have been previously demonstrated [22,25]. Besides, Cx43 expression was reduced by 40 % per unit volume of myocyte in hypertrophied myocardium from pressure-loaded human

left ventricles [17]. In addition, current study indicates that Cx43 variant phosphorylated at serine368 are significantly reduced in hypertrophied left ventricle of SHR and hyperthyroid rat hearts compared to healthy rats. It appears that reduced phosphorylation might be due to reduced availability of PKCε as shown in this study. Consequently, it may facilitate alterations in Cx43 distribution, i.e. enhanced localization on lateral plasma membrane of hypertrophied cardiomyocytes of hypertensive and hyperthyroid rat heart. Although mechanisms for these prominent changes are not comprehensively elucidated, it is hypothesized that lateralization of Cx43 and high lateral conduction contribute to decrease of anisotropic ratio and slowing of conduction [26,27].

In this context, it should be emphasized that proper Cx43 channels mediated electrical coupling and communication is essential for normal electrical activation of the myocardium, anisotropic conduction and synchronized contraction of the heart [13,14]. Thus, no doubts that significant decrease of Cx43, its 368 variant and PKCε may deteriorate electrical coupling and along with increased "side to side" conduction in hypertrophied heart [26] can cause abnormal conduction promoting generation of malignant arrhythmias [24]. It may underlie increased susceptibility to ventricular fibrillation demonstrated in SHR and hyperthyroid rat hearts [7,11].

However, unlike our expanded knowledge concern myocardial hypertrophy [7,8] much less is known about myocardial or cardiomyocyte atrophy [3]. In line with previous findings [10,11,22] the decrease of the left ventricular weight was registered in rat hearts in response to hypothyroid status and type-1 diabetes, most likely due to reduction of cardiac workload. Besides, there was a significant reduction of cross sectional area of cardiomyocytes pointing out the myocardial atrophy. The latter was accompanied by enhanced total Cx43 protein (shown also previously, [10,11,22]) as well as its variant phosphorylated at serine368 along with increase of PKCε abundance. While, atrophied cardiomyocytes did not exhibit apparent alterations in Cx43 topology, like pro-arrhythmic lateral distribution. Therefore, it can be expected that atrophied heart might be less prone to develop malignant arrhythmias, as it was demonstrated previously [10,11]. Of interest, atrophic myocytes that occur at sites of fibrosis and in the failing heart represent endogenous population, which could be rescued to recover ventricular function [3]. Moreover, atrophic signalling, concordant with hypertrophy, occurs in the presence of a reparative fibrosis [28]. Furthermore, lentivirus-mediated delivery of Cx43 into post-myocardial infarction scar enhanced conduction velocity through cardiomyocyte-myofibroblast electrical coupling within the scar and provided arrhythmia protection [29].

In the context of the presented pathophysiological models it should be noted that these are accompanied by alterations in protein synthesis but also proteolysis and these processes may account for either cardiomyocyte hypertrophy or atrophy [30]. However, it is difficult to recognize as whether the changes in Cx43 protein levels are induced by systemic disease itself or due to structural remodelling. It is supposed that both factors may be involved in protein levels of Cx43 and its topology in adaptive myocardial hypotrophy or hypertrophy.

Of interest, during postnatal development of human heart, the cardiomyocyte growth is accompanied by alterations in expression as well as topology of Cx43 [31]. These changes likely to be associated with alterations in the functional anisotropy. According to Seidel *et al.* [26], high lateral gap junction conductance and enhanced cell diameter increased the susceptibility to conduction block at tissue expansion, providing a substrate for arrhythmia.

In the context of the propensity of the heart to cardiac arrhythmias in our rat models it should be emphasized that both myocardial hypertrophy and atrophy are also accompanied by alterations/dysfunction of ion channels and Ca^{2+} handling disorders [7,9,18,32,33]. These disturbances underlie occurrence of transient arrhythmias, such as ventricular premature beats and ventricular tachycardia due to ectopic activity resulting from early or delayed after-depolarizations. While these can initiate the re-entry-mediated life-threatening ventricular tachycardia or fibrillation in the heart exhibiting pro-arrhythmia substrate encompassing impairment of Cx43 channels. Sudden cardiac death is mostly attributed to ventricular fibrillation or high frequency ventricular tachycardia resulting in hemodynamic collapse.

Conclusions

Findings of this study imply that pro-arrhythmic cardiac phenotype elicited by an increase cardiac workload of SHR and hyperthyroid rats was associated with down-regulation of Cx43-PKCε pathway along with pronounced localization of Cx43 on lateral sides of

hypertrophied cardiomyocytes. In contrast, the anti-arrhythmic phenotype elicited by reduced workload of hypothyroid and type-1 diabetic rats was associated with up-regulation of Cx43-PKCε pathway without apparent changes in Cx43 distribution in atrophied cardiomyocytes. It can be hypothesized that enhanced phosphorylation of Cx43 at serine368 by PKCε and perhaps alterations in excitability contribute to myocardial electrical stability and vice versa that should be proved in further studies.

Limitations of the study

We would like to emphasize that it is a pilot study encouraging to analyse the distinct abundance of Cx43 per volume of individual hypertrophied versus atrophied cardiomyocytes in confocal microscope. It could provide further data supporting differences in myocardial structural remodelling impacting cardiac arrhythmia susceptibility.

Conflict of Interest

There is no conflict of interest.

Acknowledgements

This study was supported by VEGA 2/0158/19, 2/0002/20, APVV 21-0410 and EU-ITMS 26230120006 grants.

References

1. Campbell SE, Korecky B, Rakusan K. Remodeling of myocyte dimensions in hypertrophic and atrophic rat hearts. Circ Res 1991;68:984-996. https://doi.org/10.1161/01.RES.68.4.984
2. Anversa P, Ricci R, Olivetti G. Quantitative structural analysis of the myocardium during physiologic growth and induced cardiac hypertrophy: A review. J Am Coll Cardiol 1986;7:1140-1149. https://doi.org/10.1016/S0735-1097(86)80236-4
3. Heckle MR, Flatt DM, Sun Y, Mancarella S, Marion TN, Gerling IC, Weber KT. Atrophied cardiomyocytes and their potential for rescue and recovery of ventricular function. Heart Fail Rev 2016;21:191-198. https://doi.org/10.1007/s10741-016-9535-x
4. Thompson EW, Marino TA, Uboh CE, Kent RL, Cooper IV G. Atrophy reversal and cardiocyte redifferentiation in reloaded cat myocardium. Circ Res 1984;54:367-377. https://doi.org/10.1161/01.RES.54.4.367
5. Montalvo D, Pérez-Treviño P, Madrazo-Aguirre K, González-Mondellini FA, Miranda-Roblero HO, Ramonfaur-Gracia D, Jacobo-Antonio M, ET AL. Underlying mechanism of the contractile dysfunction in atrophied ventricular myocytes from a murine model of hypothyroidism. Cell Calcium 2018;72:26-38. https://doi.org/10.1016/j.ceca.2018.01.005
6. Weber KT. Depressed myocardial contractility: can it be rescued? Am J Med Sci 2016;352:428-432. https://doi.org/10.1016/j.amjms.2016.05.026
7. Egan Benova T, Szeiffova Bacova B, Viczenczova C, Diez E, Barancik M, Tribulova N. Protection of cardiac cell-to-cell coupling attenuate myocardial remodeling and proarrhythmia induced by hypertension. Physiol Res 2016;65(Suppl 1):S29-S42. https://doi.org/10.33549/physiolres.933391
8. Bacharova L. Missing link between molecular aspects of ventricular arrhythmias and QRS complex morphology in left ventricular hypertrophy. Int J Mol Sci 2020;21:48. https://doi.org/10.3390/ijms21010048
9. Tribulova N, Knezl V, Shainberg A, Seki S, Soukup T. Thyroid hormones and cardiac arrhythmias. Vascul Pharmacol 2010;52:102-112. https://doi.org/10.1016/j.vph.2009.10.001
10. Lin H, Mitasikova M, Dlugosova K, Okruhlicova L, Imanaga I, Ogawa K, Weismann P, Tribulova N. Thyroid hormones suppress ε-pkc signalling, down- regulate connexin-43 and increase lethal arrhythmia susceptibility in non-diabetic and diabetic rat hearts. Physiol Pharmacol 2008;59:271-285.
11. Szeiffová Bačová B, Vinczenzová C, Žurmanová J, Kašparová D, Knezl V, Beňová TE, Pavelka S, Soukup T, Tribulová N. Altered thyroid status affects myocardial expression of connexin-43 and susceptibility of rat heart to malignant arrhythmias that can be partially normalized by red palm oil intake. Histochem Cell Biol 2017;147:63-73. https://doi.org/10.1007/s00418-016-1488-6
12. Bernjak A, Novodvorsky P, Chow E, Iqbal A, Sellors L, Williams S, Fawdry RA, ET AL. Cardiac arrhythmias and electrophysiologic responses during spontaneous hyperglycaemia in adults with type 1 diabetes mellitus. Diabetes Metab 2021;47:101237. https://doi.org/10.1016/j.diabet.2021.101237

13. Salameh A, Dhein S. Pharmacology of Gap junctions. New pharmacological targets for treatment of arrhythmia, seizure and cancer? Biochim Biophys Acta 2005;1719:36-58. https://doi.org/10.1016/j.bbamem.2005.09.007
14. Andelova K, Benova TE, Bacova BS, Sykora M, Prado NJ, Diez ER, Hlivak P, Tribulova N. Cardiac connexin-43 hemichannels and pannexin1 channels: Provocative antiarrhythmic targets. Int J Mol Sci 2021;22:1-22. https://doi.org/10.3390/ijms22010260
15. Dhillon PS, Gray R, Kojodjojo P, Jabr R, Chowdhury R, Fry CH, Peters NS. Relationship between gap-junctional conductance and conduction velocity in mammalian myocardium. Circ Arrhythmia Electrophysiol 2013;6:1208-1214. https://doi.org/10.1161/CIRCEP.113.000848
16. Dhein S, Salameh A. Remodeling of cardiac gap junctional cell-cell coupling. Cells 2021;10:2422. https://doi.org/10.3390/cells10092422
17. Peters NS. New insights into myocardial arrhythmogenesis: Distribution of gap-junctional coupling in normal, ischaemic and hypertrophied human hearts. Clin Sci 1996;90:447-452. https://doi.org/10.1042/cs0900447
18. Thomas D, Christ T, Fabritz L, Goette A, Hammwöhner M, Heijman J, Kockskämper J, ET AL. German Cardiac Society Working Group on Cellular Electrophysiology state-of-the-art paper: impact of molecular mechanisms on clinical arrhythmia management. Clin Res Cardiol 2019;108:577-599. https://doi.org/10.1007/s00392-018-1377-1
19. Bao X, Reuss L, Altenberg GA. Regulation of purified and reconstituted connexin 43 hemichannels by protein kinase C-mediated phosphorylation of serine 368. J Biol Chem 2004;279:20058-20066. https://doi.org/10.1074/jbc.M311137200
20. Benova T, Viczenczova C, Radosinska J, Bacova B, Knezl V, Dosenko V, Weismann P, ET AL. Melatonin attenuates hypertension-related proarrhythmic myocardial maladaptation of connexin-43 and propensity of the heart to lethal arrhythmias. Can J Physiol Pharmacol 2013;91:633-639. https://doi.org/10.1139/cjpp-2012-0393
21. Bacova BS, Viczenczova C, Andelova K, Sykora M, Chaudagar K, Barancik M, Adamcova M, ET AL. Antiarrhythmic effects of melatonin and omega-3 are linked with protection of myocardial cx43 topology and suppression of fibrosis in catecholamine stressed normotensive and hypertensive rats. Antioxidants 2020;9:1-19. https://doi.org/10.3390/antiox9060546
22. Sykora M, Bacova BS, Benova TE, Barancik M, Zurmanova J, Rauchova H, Weismann P, ET AL. Cardiac Cx43 and ECM responses to altered thyroid status are blunted in spontaneously hypertensive versus normotensive rats. Int J Mol Sci 2019;20:3758. https://doi.org/10.3390/ijms20153758
23. Gutstein DE, Morley GE, Vaidya D, Liu F, Chen FL, Stuhlmann H, Fishman GI. Heterogeneous expression of gap junction channels in the heart leads to conduction defects and ventricular dysfunction. Circulation 2001;104:1194-1199. https://doi.org/10.1161/hc3601.093990
24. Tribulova N, Szeiffova Bacova B, Benova T, Viczenczova C. Can we protect from malignant arrhythmias by modulation of cardiac cell-to-cell coupling? J Electrocardiol 2015;48:434-440. https://doi.org/10.1016/j.jelectrocard.2015.02.006
25. Szeiffová Bačova B, Egan Beňová T, Viczenczová C, Soukup T, Raučhová H, Pavelka S, Knezl V, Barancík M, Tribulová N. Cardiac connexin-43 and PKC signaling in rats with altered thyroid status without and with omega-3 fatty acids intake. Physiol Res 2016;65(Suppl 1):S77-S90. https://doi.org/10.33549/physiolres.933413
26. Seidel T, Salameh A, Dhein S. A simulation study of cellular hypertrophy and connexin lateralization in cardiac tissue. Biophys J 2010;99:2821-2830. https://doi.org/10.1016/j.bpj.2010.09.010
27. Duffy HS. The molecular mechanisms of gap junction remodeling. Hear Rhythm 2012;9:1331-1334. https://doi.org/10.1016/j.hrthm.2011.11.048
28. Kamalov G, Zhao W, Zhao T, Sun Y, Ahokas RA, Marion TN, Al Darazi F, ET AL. Atrophic cardiomyocyte signaling in hypertensive heart disease. J Cardiovasc Pharmacol 2013;62:497-506. https://doi.org/10.1097/FJC.0000000000000011
29. Roell W, Klein AM, Breitbach M, Becker TS, Parikh A, Lee J, Zimmermann K, ET AL. Overexpression of Cx43 in cells of the myocardial scar: Correction of post-infarct arrhythmias through heterotypic cell-cell coupling. Sci Rep 2018;8:1-14. https://doi.org/10.1038/s41598-018-25147-8
30. Szeiffova Bacova B, Andelova K, Sykora M, Egan Benova T, Barancik M, Kurahara LH, Tribulova N. Does myocardial atrophy represent anti-arrhythmic phenotype? Biomedicines 2022;10:2819. https://doi.org/10.3390/biomedicines10112819

31. Peters NS, Severs NJ, Rothery SM, Lincoln C, Yacoub MH, Green CR. Spatiotemporal relation between gap junctions and fascia adherens junctions during postnatal development of human ventricular myocardium. Circulation 1994;90:713-725. https://doi.org/10.1161/01.CIR.90.2.713
32. Ravingerova T, Stetka R, Barancik M, Volkovova K, Pancza D, Ziegelhöffer A, Styk J. Response to ischemia and endogenous myocardial protection in the diabetic heart. Adv Exp Med Biol 2001;498:285-293. https://doi.org/10.1007/978-1-4615-1321-6_36
33. Hegyi B, Ko CY, Bossuyt J, Bers DM. Two-hit mechanism of cardiac arrhythmias in diabetic hyperglycaemia: Reduced repolarization reserve, neurohormonal stimulation, and heart failure exacerbate susceptibility. Cardiovasc Res 2021;117:2781-2793. https://doi.org/10.1093/cvr/cvab006